

# Parametric Study of Proton-Implanted Photonic Crystal Vertical-Cavity Surface-Emitting Lasers

Paul O. Leisher, *Student Member, IEEE*, Joshua D. Sulkin, *Student Member, IEEE*,  
and Kent D. Choquette, *Fellow, IEEE*

**Abstract**—Photonic crystals with single- and seven-point defects are used to achieve single-fundamental-mode operation of proton-implanted vertical-cavity surface-emitting lasers. The holes are etched at a variety of depths for various photonic crystal designs to investigate the influence on single-mode emission. Because proton-implantation provides weak transverse confinement in the form of thermal lensing, selective loss is not required to suppress lasing of extended photonic crystal modes. We show that etching the photonic crystals to shallow depths provides the ability to scale to large aperture sizes, while etching deeply allows single-mode emission of small diameter devices. Optimized designs exhibit a net reduction in loss relative to unetched control devices, as evidenced by a reduction in device threshold current.

**Index Terms**—Distributed Bragg reflector lasers, photonic crystals, semiconductor lasers, vertical-cavity surface-emitting lasers (VCSELs).

## I. INTRODUCTION

FUNDAMENTAL mode operation of vertical-cavity surface-emitting lasers (VCSELs) is desired for numerous applications including high-speed fiber optic data communication, sensing, computer mice, and compact atomic clocks. VCSELs offer a number of potential benefits over Fabry–Perot semiconductor lasers such as capability for on-wafer testing, single longitudinal mode operation, high-speed operation, and low-cost high-volume manufacturability. Unfortunately, all but the smallest diameter oxide- and implant-confined VCSELs tend to operate in multiple transverse modes. Increasing the aperture size to achieve higher output powers while maintaining single-mode operation has provided a unique set of challenges.

Recently, there has been considerable interest in achieving a low-cost scalable method of designing single-mode VCSELs. Methods such as the use of small diameter oxide [1], implant [2], or hybrid oxide-implant apertures [3], and etched surface reliefs [4], [5] have shown success, but require stringent design tolerances. There has also been considerable interest in the use of etched structures such as photonic crystals [6]–[11] and non-periodic holes (such as wedges) [12]–[14] to achieve scalable single-mode results. The photonic crystal approach is unique in

its “endlessly single-mode” property [15], which can provide single-fundamental-mode emission with a specific structure independent of wavelength.

In recent years, manufacture of VCSELs has been shifting from implant-confinement to oxide-confinement due to inherent cold-cavity index confinement, which results in improved device performance (such as lower threshold, higher efficiency, and higher power) [16]. These enhancements in device performance come at the cost of increased parasitic capacitance, which limits high-speed operation. Because etched photonic crystals (and other holey structures) provide built-in transverse index confinement, implant-confined VCSELs may benefit from their use. The use of implant confinement also offers two other distinct advantages. Implant-confined VCSELs tend to operate in the fundamental mode at threshold, and lase in only a few higher order modes at higher injection levels [2], [16]. In addition, because proton-implanted apertures provide no cold-cavity index confinement [17], the electrical and optical confinement of an implant-confined photonic crystal VCSEL can be separately controlled. The use of etched photonic crystals [10] and other holey structures [13], [14] in proton-implanted VCSELs has only recently been reported.

To date, there has been no parametric study of photonic crystal design and etch depth on single-mode performance of implant-confined VCSELs. Such a study would be useful for optimizing the designs to enable improved performance. In this paper, implant-confined photonic crystal VCSELs with varying designs were designed, fabricated, and characterized to investigate both the feasibility and scalability of the photonic crystal approach for single-mode emission. The observed modal properties of these devices are presented, and the loss effects (in the context of slope efficiency and threshold current) as a function of photonic crystal design are discussed.

## II. EXPERIMENT

The implant-confined photonic crystal VCSELs in this paper were fabricated as follows. A bottom  $n$ -type (Si-doped) 34-period distributed Bragg reflector (DBR) consisting of alternating layers of  $\text{Al}_{0.12}\text{Ga}_{0.88}\text{As}$  and  $\text{Al}_{0.90}\text{Ga}_{0.10}\text{As}$ , an undoped active region with two GaAs quantum wells, and a similar top  $p$ -type (C-doped) 21-period DBR, were grown by metalorganic vapor phase epitaxy for a designed operating wavelength of 850 nm. Ohmic ring contacts (Ti/Au) for the top  $p$ -type DBR were patterned using photolithography, deposited by electron-beam evaporation, and formed using conventional liftoff. A backside contact (AuGe/Ni/Au) was deposited to form an ohmic contact to the  $n$ -type substrate. A thin protective layer of  $\text{SiO}_2$

Manuscript received November 7, 2006; revised July 10, 2007. This work was supported by the National Science Foundation under Grant 03-35082.

P. O. Leisher was with the Micro and Nanotechnology Laboratory, Department of Electrical and Computer Engineering, University of Illinois at Urbana-Champaign, Urbana, IL 61801 USA. He is now with nLight Corporation, Vancouver, WA 98665 USA (e-mail: pleisher@ieee.org).

J. D. Sulkin and K. D. Choquette are with the Micro and Nanotechnology Laboratory, Department of Electrical and Computer Engineering, University of Illinois at Urbana-Champaign, Urbana, IL 61801 USA (e-mail: sulkin@uiuc.edu; choquett@uiuc.edu).

Digital Object Identifier 10.1109/JSTQE.2007.905330

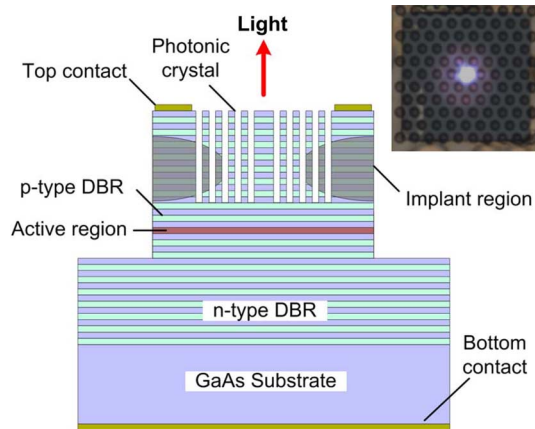


Fig. 1. Cross-sectional schematic of an implant-confined photonic crystal VCSEL. The inset depicts a near-field optical microscopic image of a typical device lasing in the fundamental mode.

was deposited, and thick ( $12\ \mu\text{m}$ ) photoresist pillars were patterned in the center of each top ring contact. The exposed  $\text{SiO}_2$  was etched using  $\text{CF}_4$  reactive ion etching (RIE). These pillars served to mask and define the apertures for the implant process. Protons were implanted at 340 keV with a dose of  $4 \times 10^{14}\ \text{cm}^{-2}$ , and the mask was subsequently removed. Electron beam lithography was used to define the photonic crystal patterns in polymethyl-methacrylate resist, and  $\text{CHF}_3$  RIE was used to transfer the pattern to an  $\text{SiO}_2$  mask. Large isolation mesas were patterned with conventional lithography and similarly transferred to the  $\text{SiO}_2$  mask. The sample was then cleaved into smaller pieces. The isolation mesas and the photonic crystal holes were simultaneously etched into the top DBR using  $\text{SiCl}_4/\text{Ar}$  inductively coupled plasma RIE. Each sample was etched for a different time, resulting in variety of etch depths for each photonic crystal design. The oxide mask was removed by  $\text{CF}_4$  RIE, and the samples were subjected to 30 s of rapid thermal annealing at  $325\ ^\circ\text{C}$ . Fig. 1 illustrates a schematic of a completed implant-confined photonic crystal VCSEL, with an inset showing a completed device lasing in the fundamental mode.

Here, the ion implant aperture diameter was fixed at  $20\ \mu\text{m}$ . The photonic crystal lattice spacing is given by  $a$  and the hole diameter  $b$ . The photonic crystals were designed with  $b/a = 0.4, 0.5, 0.6,$  and  $0.7$ , and  $a$  was varied from  $2.0$  to  $12.5\ \mu\text{m}$  (in steps of  $0.5\ \mu\text{m}$ ) for single-point defect designs, and from  $1.0$  to  $6.0\ \mu\text{m}$  (in steps of  $0.5\ \mu\text{m}$ ) for seven-point defect designs. The etch depth for the four samples (referred to as Samples A, B, C, and D) was investigated as a function of photonic crystal hole diameter ( $b$ ), as shown in Fig. 2. The holes were inspected in a scanning electron microscope at an angle of  $35^\circ$  off-normal, and the etch depth was calculated by counting the number of DBR periods etched and multiplying by the thickness of one period. For a given etching time, the smaller diameter holes etched to a shallower depth. This dependence is attributed to size-dependent etch effects [18]. The etch-depth data was empirically fit with a logarithmic function for the purpose of interpolating etch depths for all devices in the paper.

The characteristics of each VCSEL were measured using on-wafer probing at room temperature. For continuous-wave (CW)

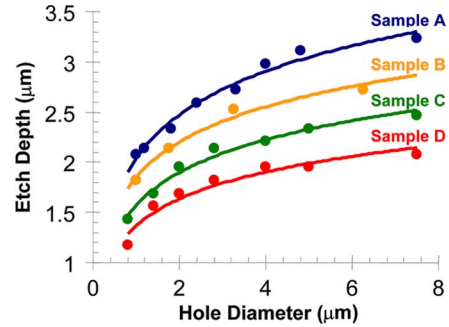


Fig. 2. Etch depth as a function of hole diameter  $b$  for the four samples. For each sample, the data is empirically fit with a logarithmic function.

light versus current ( $LI$ ) and current versus voltage ( $IV$ ) measurements, the input current was varied, and both the device voltage and the output from a silicon photodetector were measured using a semiconductor parameter analyzer. The spectral characteristics were measured using an optical spectrum analyzer with resolution bandwidth of  $0.06\ \text{nm}$ . At maximum power, each VCSEL was categorized as either not lasing, multimode lasing, or single-mode lasing, where single mode is defined as a single peak at the fundamental (lowest energy) wavelength and greater than  $30\ \text{dB}$  side mode suppression ratio (SMSR) over the entire dynamic operating range of the VCSEL. Multimode lasing would be a higher order defect-confined mode, rather than a photonic crystal mode extended across the defect and photonic crystal.

### III. RESULTS

The modal properties of a lossless cylindrical step-index waveguide can be predicted using the  $V$ -parameter, which is given by [19]

$$V_{\text{eff}} = \frac{\pi D}{\lambda_o} \sqrt{n_1^2 - n_2^2}. \quad (1)$$

where the wavelength of operation is  $\lambda_o$ , and the waveguide diameter  $D$  is the photonic crystal defect diameter  $2a - b$ . The “core” index  $n_1$  is given by the effective index of the un-etched DBR in the defect, and the “clad” index  $n_2$  is the overall effective index of the etched photonic crystal. Because the photonic crystal is etched into the semiconductor DBR composed of layers with periodically varying refractive index, an accurate computation of  $V_{\text{eff}}$  for a photonic crystal VCSEL, which takes into account finite etching depth, requires a layer-by-layer calculation of the out-of-plane photonic band diagram to obtain the index contrast. The details of this procedure were originally outlined in [8]. If  $V_{\text{eff}}$  is less than 2.4, and the corresponding index contrast is sufficient to dominate over thermal lensing ( $n_1 - n_2 > 10^{-3}$ ), the device is expected to operate in the single fundamental mode [8], [9].

Fig. 3(a) illustrates the spectrum of a typical single-mode device in this study, taken at an injection level corresponding to maximum output power (thermal rollover). This particular data comes from a single-point defect device on Sample C with photonic crystal parameters  $b/a = 0.6$  and  $a = 5.0\ \mu\text{m}$  (defect diameter =  $7\ \mu\text{m}$ ), which corresponds to a calculated  $V_{\text{eff}} = 2.1$ .

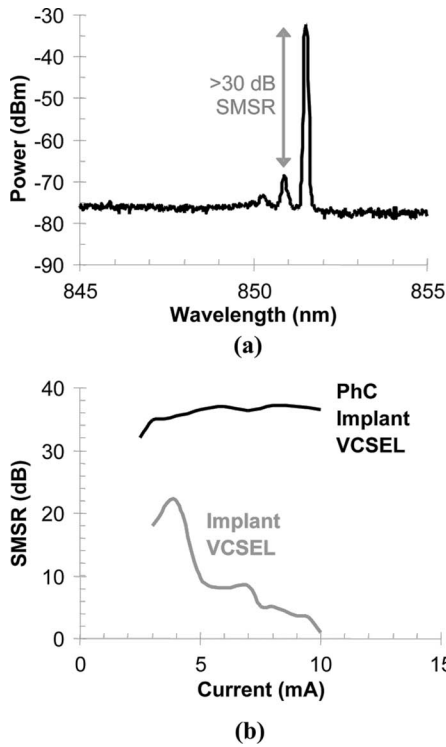


Fig. 3. (a) Typical single-mode spectrum for an implant-confined photonic crystal VCSEL at maximum power. (b) SMSR as a function of injection current for the same laser. The values for an unetched control laser with the same implant aperture size have been plotted for reference.

Fig. 3(b) shows the SMSR as a function of drive current for the photonic crystal device. The behavior for an unetched control ( $20\ \mu\text{m}$  implant diameter) device is plotted on the same graph for comparison. Single-mode implanted VCSELs would be expected for implant diameters smaller than  $5\ \mu\text{m}$ .

Fig. 4(a) shows the CW  $LI$  for the same device. This device exhibits a threshold current of  $1.7\ \text{mA}$ , a slope efficiency of  $0.28\ \text{W/A}$ , and a maximum single-mode output of  $1.5\ \text{mW}$ . The CW  $LI$  for an unetched control having the same implant diameter is also plotted in the same figure for comparison. The reduction in threshold current and increase in efficiency in the photonic crystal device is due to a decrease in diffraction loss resulting from the index confinement provided by the photonic crystal. The CW  $IV$  curves for the photonic crystal and unetched control VCSELs are shown in Fig. 4(b). The increased series resistance in the photonic crystal VCSEL is due to the removal of conductive material.

The dependence of threshold current and slope efficiency on photonic crystal design for the single-mode single-point defect devices on Sample C is shown in Fig. 5(a) and (b), respectively. The observed increase in slope efficiency and decrease in threshold current for increasing defect diameters is a direct consequence of decreasing diffraction loss. For a given  $b/a$ , the defect diameter increases by increasing the hole diameter  $b$ . This increased hole diameter results in a deeper etch depth, and consequently, larger effective index contrast, which is responsible for the decreased diffraction loss.

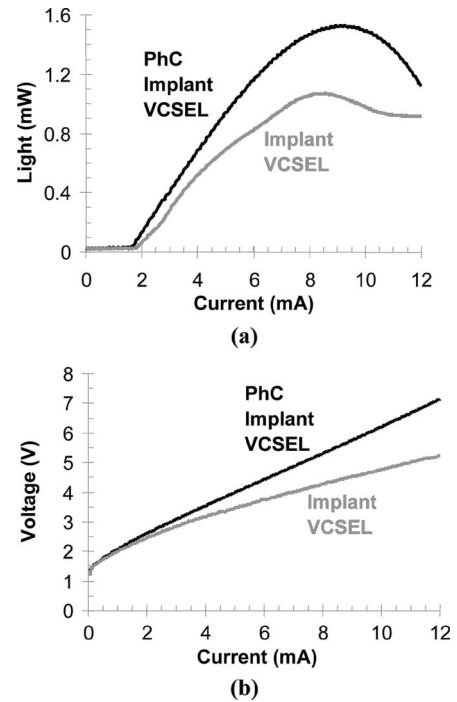


Fig. 4. (a) Output power and (b) voltage versus injection current for the same VCSEL described in Fig. 3, and an unetched control laser with the same implant aperture size.

The modal properties for all devices (single- and seven-point defects) in the paper were collected and compiled in Fig. 6. For each device,  $V_{\text{eff}}$  was calculated and the measured modal property was determined versus the defect aperture size. Single-mode results were obtained for defect diameters between  $4$  and  $9\ \mu\text{m}$ . Devices with defect diameters smaller than  $4\ \mu\text{m}$  did not generally lase. These devices had the smallest photonic crystal hole sizes with relatively shallow etch depths, and thus, they were insufficiently etched to provide enough index confinement to achieve threshold (too much diffraction loss). Devices with defect diameters larger than  $9\ \mu\text{m}$  lased multimode due to thermal instabilities in the defect aperture. A number of devices with calculated  $V_{\text{eff}}$  values above  $2.4$  operated single mode due to loss introduced by the holes, which is not included in the computation of  $V_{\text{eff}}$ . These results are comparable to those obtained for the oxide-confined photonic crystal VCSELs in [11], indicating that the use of photonic crystals for single-mode emission in VCSELs is compatible with a variety of current injection schemes.

Fig. 7 illustrates the inherent tradeoff between aperture diameter and etch depth (index contrast) for single-mode emission of single-point defect devices, which is a direct result of (1). Single-mode results for shallow etch depths are obtained for larger defect diameters relative to the single-mode results for deeper etch depths. The use of shallow etch depths should allow scaling of the single-mode single-point defect diameters greater than  $10\ \mu\text{m}$ . The ability to scale to shallow etch depths is unique to implant-confined photonic crystal VCSELs. In contrast, oxide-confined photonic crystal VCSELs require a minimum hole etch depth to provide sufficient loss in order to inhibit lasing of the strongly guided oxide modes [11]. Fig. 7 also shows that deeply

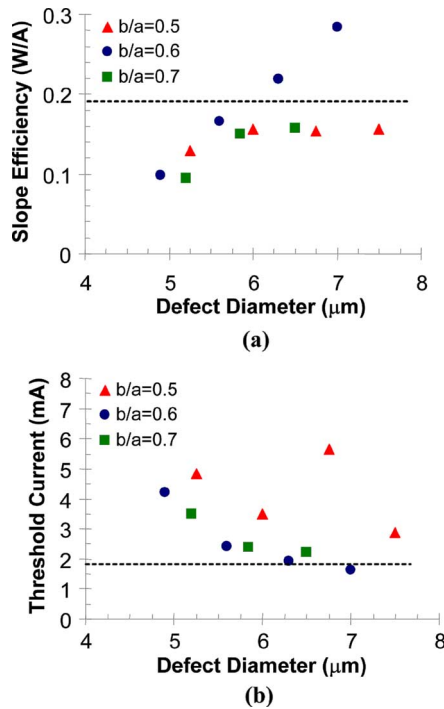


Fig. 5. (a) Threshold current and (b) slope efficiency as a function of the photonic crystal defect aperture size for single-mode single-point defect devices on Sample C. The dotted lines indicate the average values for an unetched control device with the same implant aperture size.

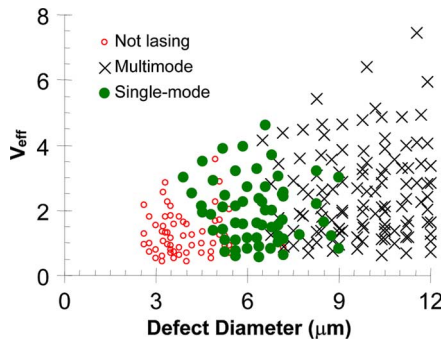


Fig. 6. Observed modal properties as a function of photonic crystal defect diameter for implant-confined photonic crystal VCSELs.

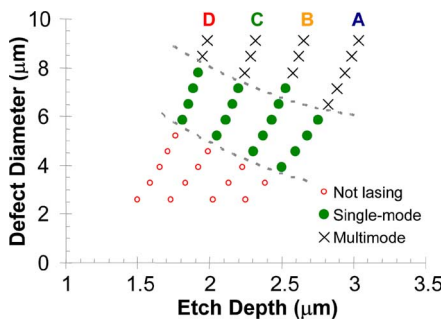


Fig. 7. Observed modal properties as a function of defect diameter and etch depth (index contrast) for implant-confined photonic crystal VCSELs.

etched holes will enable small diameter lasers, although the high aspect ratio etching required (small diameter and deep depth) may prove challenging. A hybrid mirror design [20] would be advantageous for small diameter photonic crystal VCSELs.

#### IV. CONCLUSION

Implant-confined photonic crystal VCSELs were designed, fabricated, and characterized to parametrically study the effects of photonic crystal design and etch depth on single-mode operation. Because proton-implantation provides weak transverse confinement in the form of thermal lensing, selective loss is not required to suppress the lasing of extended modes. We show that etching the photonic crystals to shallow depths provides the ability to scale to large aperture sizes. Optimized designs exhibit a net reduction in loss relative to unetched control devices, as evidenced by a reduction in device threshold current and improved efficiency. Future work will focus on reducing the implant aperture size to form a more optimum overlap of the electrical and implant apertures in an effort to improve the device efficiency, as well as reducing the photonic crystal etch depth in an effort to scale to larger optical aperture sizes for high-power operation.

#### ACKNOWLEDGMENT

The authors would like to thank A. J. Danner.

#### REFERENCES

- [1] C. Jung, R. Jäger, M. Grabherr, P. Schnitzer, R. Michalzik, B. Weigl, S. Müller, and K. J. Ebeling, "4.8 mW singlemode oxide confined top-surface emitting vertical-cavity laser diodes," *Electron. Lett.*, vol. 33, no. 21, pp. 1790–1791, Oct. 1997.
- [2] R. A. Morgan, G. D. Guth, M. W. Focht, M. T. Asom, K. Kojima, L. E. Rogers, and S. E. Callis, "Transverse mode control of vertical-cavity top-surface-emitting lasers," *IEEE Photon. Technol. Lett.*, vol. 4, no. 4, pp. 374–377, Apr. 1993.
- [3] E. W. Young, K. D. Choquette, S. L. Chuang, K. M. Geib, A. J. Fischer, and A. A. Allerman, "Single-transverse-mode vertical-cavity lasers under continuous and pulsed operation," *IEEE Photon. Technol. Lett.*, vol. 13, no. 9, pp. 927–929, Sep. 2001.
- [4] H. Martinsson, J. A. Vukusic, M. Grabherr, R. Michalzik, R. Jäger, K. J. Ebeling, and A. Larsson, "Transverse mode selection in large-area oxide-confined vertical-cavity surface-emitting lasers using a shallow surface relief," *IEEE Photon. Technol. Lett.*, vol. 11, no. 12, pp. 1536–1538, Dec. 1999.
- [5] H. J. Unold, S. W. Z. Mahmoud, R. Jäger, M. Kicherer, M. C. Riedl, and K. J. Ebeling, "Improving single-mode VCSEL performance by introducing a long monolithic cavity," *IEEE Photon. Technol. Lett.*, vol. 12, no. 8, pp. 939–941, Aug. 2000.
- [6] D. S. Song, S. H. Kim, H. G. Park, C. K. Kim, and Y. H. Lee, "Single-fundamental-mode photonic-crystal vertical-cavity surface-emitting lasers," *Appl. Phys. Lett.*, vol. 80, pp. 3901–3903, 2002.
- [7] N. Yokouchi, A. J. Danner, and K. D. Choquette, "Two-dimensional photonic crystal confined vertical-cavity surface-emitting lasers," *IEEE J. Sel. Topics Quantum Electron.*, vol. 9, no. 5, pp. 1439–1445, Sep./Oct. 2003.
- [8] N. Yokouchi, A. J. Danner, and K. D. Choquette, "Etching depth dependence of the effective refractive index in two-dimensional photonic-crystal-patterned vertical-cavity surface-emitting laser structures," *Appl. Phys. Lett.*, vol. 82, no. 9, pp. 1344–1346, 2003.
- [9] J. Danner, J. J. Raftery Jr., T. Kim, P. O. Leisher, A. V. Giannopoulos, and K. D. Choquette, "Progress in photonic crystal vertical cavity lasers," *IEICE Trans. Electron.*, vol. E88-C, no. 5, pp. 944–950, 2005.
- [10] H. P. D. Yang, F. I. Lai, Y. H. Chang, H. C. Yu, C. P. Sung, H. C. Kuo, S. C. Wang, S. Y. Lin, and J. Y. Chi, "Singlemode (SMSR > 40 dB) proton-implanted photonic crystal vertical-cavity surface emitting lasers," *Electron. Lett.*, vol. 41, no. 6, pp. 326–328, Mar. 2005.

- [11] J. Danner, J. J. Raftery Jr., P. O. Leisher, and K. D. Choquette, "Single mode photonic crystal vertical cavity lasers," *Appl. Phys. Lett.*, vol. 88, pp. 091114-1–091114-3, 2006.
- [12] A. Furukawa, S. Sasaki, M. Hoshi, A. Matsuzono, K. Moritoh, and T. Baba, "High-power single-mode vertical-cavity surface-emitting lasers with triangular holey structure," *Appl. Phys. Lett.*, vol. 85, pp. 5161–5163, 2004.
- [13] P. O. Leisher, A. J. Danner, J. J. Raftery Jr., and K. D. Choquette, "Proton implanted single mode holey vertical-cavity surface emitting lasers," *Electron. Lett.*, vol. 41, no. 18, pp. 1010–1011, Sep. 2005.
- [14] P. O. Leisher, A. J. Danner, J. J. Raftery Jr., D. F. Siriani, and K. D. Choquette, "Loss and index guiding in single mode proton-implanted holey vertical-cavity surface-emitting lasers," *IEEE J. Quantum Electron.*, vol. 42, no. 10, pp. 1091–1096, Oct. 2006.
- [15] T. A. Birks, J. C. Knight, P. St. and J. Russell, "Endlessly single-mode photonic crystal fiber," *Opt. Lett.*, vol. 22, pp. 961–963, 1997.
- [16] K. D. Choquette and K. M. Geib, "Fabrication and performance of vertical-cavity surface-emitting lasers," in *Vertical-Cavity Surface-Emitting Lasers*, C. W. Wilmsen, H. Temkin, and L. A. Coldren, Eds. New York: Cambridge Univ. Press, 1999, pp. 193–232.
- [17] N. K. Dutta, L. W. Tu, G. Hasnain, G. Zydzik, Y. H. Wang, and A. Y. Cho, "Anomalous temporal response of gain guided surface emitting lasers," *Electron. Lett.*, vol. 27, no. 3, pp. 208–210, Jan. 1991.
- [18] R. A. Gottscho and C. W. Jurgensen, "Microscopic uniformity in plasma etching," *J. Vacuum Sci. Technol. B*, vol. 10, no. 5, pp. 2133–2143, 1992.
- [19] D. Gloge, "Weakly guiding fibers," *Appl. Opt.*, vol. 10, no. 10, pp. 2252–2258, 1971.
- [20] P. O. Leisher, A. J. Danner, and K. D. Choquette, "Single mode 1.3  $\mu\text{m}$  photonic crystal vertical-cavity surface-emitting laser," *IEEE Photon. Technol. Lett.*, vol. 18, no. 20, pp. 2156–2158, Oct. 2006.



**Paul O. Leisher** (S'98) received the B.S. degree in electrical engineering from Bradley University, Peoria, IL, in 2002, and the M.S. and Ph.D. degrees in electrical and computer engineering from the University of Illinois at Urbana-Champaign, Urbana, in 2004 and 2007, respectively.

In 2007, he joined nLight Corporation, Vancouver, WA, where he is currently a Device Engineer. His research interests include design, fabrication, characterization, and analysis of semiconductor lasers and other photonic devices. He has

authored more than 50 papers published in technical journals and conference proceedings.

Dr. Leisher is a member of the IEEE Lasers and Electro-Optics Society and the Optical Society of America.



**Joshua D. Sulkin** (S'02) received the B.S. degree in computer engineering from the University of Illinois at Urbana-Champaign, Urbana, in 2006, where he is currently working toward the M.S. degree in electrical engineering.

He joined the Photonic Device Research Group as an undergraduate Research Assistant affiliated with the Center for Nanoscale Chemical-Electrical-Mechanical Systems, University of Illinois at Urbana-Champaign. His research interests include photonic devices, such as vertical-cavity surface-emitting

lasers, and their integration with microfluidic networks for sensing and manufacturing applications.



**Kent D. Choquette** (M'97–SM'02–F'03) received the B.S. degree in engineering physics and applied mathematics from the University of Colorado, Boulder, in 1984, and the M.S. and Ph.D. degrees in materials science from the University of Wisconsin-Madison, Madison, in 1985 and 1990, respectively.

He was a Postdoctoral Researcher with AT&T Bell Laboratories, Murray Hill, NJ, in 1990. He joined Sandia National Laboratories, Albuquerque, NM, as a Postdoctoral Researcher in 1992, where he became a Principal Member of Technical Staff in 1993. He

was a Professor in the Electrical and Computer Engineering Department, University of Illinois at Urbana-Champaign, Urbana, in 2000, where he became the acting Director of the Micro and Nanotechnology Laboratory in July 2005. His research interests include design, fabrication, characterization, and applications of vertical-cavity surface-emitting lasers (VCSELs), novel microcavity light sources, nanofabrication technologies, and hybrid integration techniques. He has authored more than 200 technical publications and three book chapters, and has presented numerous invited talks and tutorials on VCSELs.

Dr. Choquette is a Fellow of the IEEE Lasers and Electro-Optics Society and the Optical Society of America. From 2000 to 2002, he was an IEEE/Lasers and Electro-Optics Society (LEOS) Distinguished Lecturer. He was an Associate Editor of the IEEE JOURNAL OF QUANTUM ELECTRONICS and IEEE PHOTONIC TECHNOLOGY LETTERS, and a Guest Editor of IEEE JOURNAL OF SELECTED TOPICS IN QUANTUM ELECTRONICS.